

# Fast, high precision dynamics in quantum optimal control theory

Mogens Dalgaard<sup>1</sup> and Felix Motzoi<sup>2,\*</sup>

<sup>1</sup>*Department of Physics and Astronomy, Aarhus University, Ny Munkegade 120, 8000 Aarhus C, Denmark*

<sup>2</sup>*Forschungszentrum Jülich, Institute of Quantum Control (PGI-8), D-52425 Jülich, Germany*

(Dated: October 13, 2021)

Quantum optimal control theory is becoming increasingly crucial as quantum devices become more precise, but the need to quickly optimize these systems classically remains a significant bottleneck in their operation. Here we present a new theoretical quantum control framework for much faster optimization than the state of the art by replacing standard time propagation with a product of short-time propagators, each calculated using the Magnus expansion. The derived formulas for exact series terms and their gradients, based on earlier approximations of the integrals in a simulation setting, allow us to subsume the high cost of calculating commutators and integrals as an initial overhead, thereby providing a tenfold speedup for all subsequent dynamical trajectories from control and noise sampling.

## I. INTRODUCTION

Quantum technologies may solve societally relevant problems within areas such as optimization [1], equation solving [2], drug design [3, 4], and machine learning [5, 6] in combinatorially difficult regimes where classical computers are expected to fail [7]. In recent years, we have witnessed the small-scale implementation of some of these ideas [8–12]. However, large-scale implementations still require significant improvement in our ability to accurately simulate and control subparts of these systems.

Quantum control optimization is formally treated within quantum control theory [13–15], where recent progress includes: frequency domain optimization [16–18], Hessian-based optimization [19–21], optimization of many-body matrix product states [11, 22], noise-resilient control [23–27], reinforcement learning-based optimization [28–34], circuit optimization [35–37], feedback control [38–41], and global cost functional landscape optimization [10, 42, 43].

One area of simulation and optimization that still has significant room for improvement is the time-dependent, controlled evolution [44]. For this purpose, a widely used analytical method is the Magnus expansion [45–48], which benefits from significantly better convergence properties than, e.g., Taylor or Dyson series. However, like these other series, going beyond a few orders is computationally (or analytically) taxing, while lower-order results only provide approximate solutions. Thus, so far, the Magnus expansion has found limited use for high precision optimal control.

In this work, we demonstrate a new numerical integration method suitable for quantum optimal control based on the Magnus expansion, which may significantly improve standard quantum optimal control integration techniques. In this context, we use the Magnus expansion, not over the entire time evolution (which is inac-

curate), but resolve it into shorter, high-accuracy time intervals [46], as is also standard for other high precision integration methods. Another crucial insight in this regard is the ability to pre-calculate commutators and integrals, allowing for the fast inclusion of higher-order terms in the Magnus expansion. Moreover, this allows each integral term in the expansion to be calculated exactly without resorting to sampling methods which further improves the precision.

For standard “single-shot” simulations, the overhead in calculating the commutators can be quite significant, making Magnus-based integration rarely more efficient than other frequently used integration techniques. However, we demonstrate that this overhead can be insignificant for optimization, and the improved convergence leads to a fairly consistent ten-fold improvement in efficiency. In particular, we demonstrate that our methodology works well for both slow and fast dynamics.

As a testbed for our methods, we optimize the global control of an Ising-type spin chain, recently studied also in Refs. [27, 43]. Locally interacting spin systems are compelling to study because of their importance within solid-state physics [49]. In addition, many quantum computational architectures depend on adjacently coupled qubits [50–54], while also having potential applications in surface error correction codes [55, 56] and transport of quantum information [57, 58].

We organize this paper as follows: In Section II we demonstrate how to use the Magnus expansion to derive different integration schemes and how to utilize these for quantum control optimization. In Section III, we benchmark these against each other with respect to both speed and accuracy. In Section IV, we present concluding remarks.

## II. THEORY

Quantum control optimization allows for shaping externally applied control fields in order to realize dynamical operations such as state-to-state transfers, unitary gate synthesis, or preparation of a density matrix in both

\* f.motzoi@fz-juelich.de

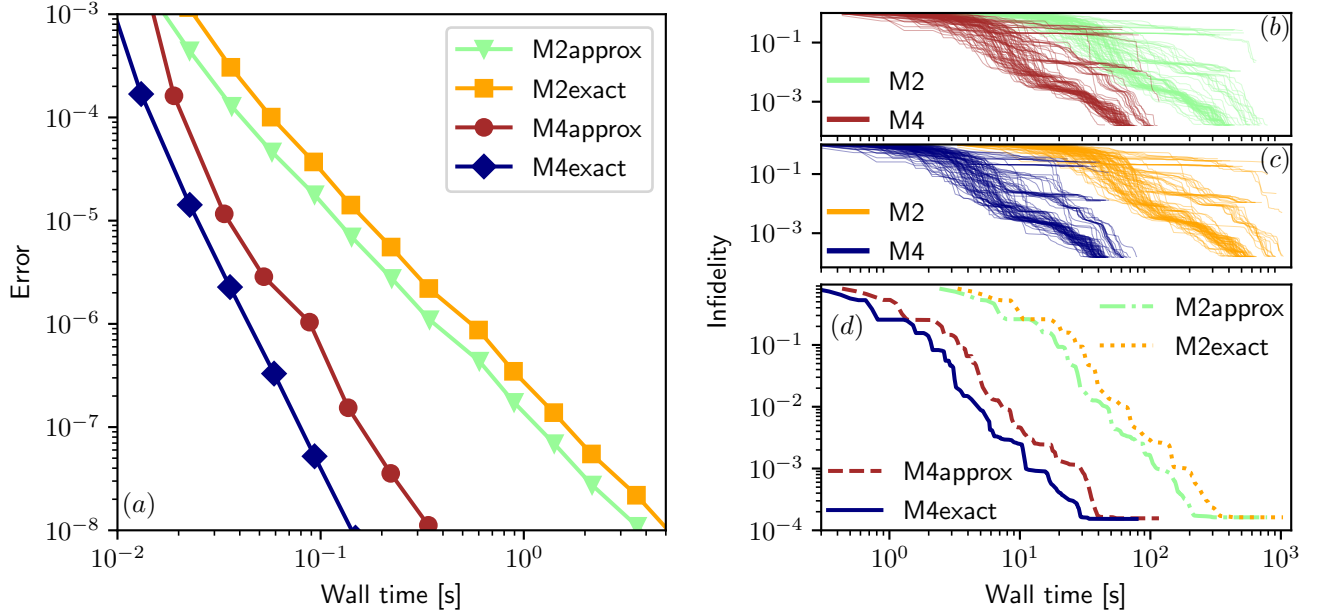


FIG. 1. (a) The wall time consumption for calculating the infidelity versus the numerical error of the infidelity averaged over 100 optimized pulses for the different methods presented in the text. We obtained the data by scanning over different values of  $\Delta t$ , see Fig. 3(a). From this data, we find the  $\Delta t$  that leads to an average error of  $10^{-6}$ . In (b), we compare the optimization from the found discretization of the two approximation methods. We repeat in (c) the comparison for the two exact methods. Finally, in (d), we depict the smallest infidelity found at each wall time duration for each of the different methods.

closed and open quantum systems [59]. One of the most successful approaches in this regard, is the gradient pulse engineering algorithm (GRAPE) [60, 61] and its many extensions [19, 20, 44, 62, 63]. The general idea is to reformulate the control problem as a minimization task of a cost-function  $\mathcal{F}[u^{(k)}]$  with respect to a set of control fields  $\{u^{(k)}\}_k$  that steers the system via a control Hamiltonian

$$H(t) = H_0 + \sum_k u^{(k)}(t)H_k. \quad (1)$$

Here  $H_0$  and  $H_k$  denote drift and control Hamiltonians, respectively, which we assume are time-independent. In this work, we specifically seek to optimize pulses expressed in a set of basis functions  $u^k(t) = \sum_n b_n^{(k)} \phi_n^{(k)}(t)$ . This type of parametrization has been popularized in literature through the chopped random basis approach [17, 18, 44, 63–65], which is suitable to obtain pulses that are easy to implement experimentally with vanishing effects [17] of filtering. With this parametrization, we now seek to minimize the cost-function  $\mathcal{F}(\{b_n^{(k)}\})$  over the pulse parameters  $\{b_n^{(k)}\}$ .

We may numerically solve, e.g., the Schrödinger equation for a duration  $T$  in a series of  $N$  equidistant steps,  $\Delta t = T/N$ , via the time evolution operator  $U(\Delta t, t) |\psi(t)\rangle = |\psi(t + \Delta t)\rangle$ . The time evolution operator for the  $j$ th time step  $t_j = j\Delta t$  is formally given by  $U(\Delta t, t_{j-1}) = U_j = e^{-i\Omega_j}$ , where  $\Omega_j = \sum_{n=1}^{\infty} \Omega_j^{[n]}$  denotes the Magnus expansion [45, 46], where the first

term reads

$$\Omega_j^{[1]} = \int_{t_j}^{t_j + \Delta t} dt_1 H(t_1) = \Delta t H_0 + \sum_k c_{k,j}^{(1)} H_k. \quad (2)$$

Note in the above equation we have inserted Eq. (1) and implicitly carried out the integral

$$c_{k,j}^{(1)} = \int_{t_j}^{t_j + \Delta t} dt_1 u^{(k)}(t_1) \quad (3)$$

The second term in the Magnus expansion reads

$$\begin{aligned} \Omega_j^{[2]} &= -\frac{i}{2} \int_{t_j}^{t_j + \Delta t} dt_1 \int_{t_j}^{t_1} dt_2 [H(t_2), H(t_1)] \\ &= -i \sum_k c_{k,j}^{(2)} [H_0, H_k] - i \sum_{k < k'} c_{k,k',j}^{(3)} [H_k, H_{k'}], \end{aligned} \quad (4)$$

where we similarly to before have collected the integrals

$$c_{k,j}^{(2)} = \frac{1}{2} \int_{t_j}^{t_j + \Delta t} dt_1 \int_{t_j}^{t_1} dt_2 (u^{(k)}(t_1) - u^{(k)}(t_2)) \quad (5)$$

$$\begin{aligned} c_{k,k',j}^{(3)} &= \frac{1}{2} \int_{t_j}^{t_j + \Delta t} dt_1 \int_{t_j}^{t_1} dt_2 \left( u^{(k)}(t_2) u^{(k')}(t_1) \right. \\ &\quad \left. - u^{(k')}(t_2) u^{(k)}(t_1) \right). \end{aligned} \quad (6)$$

Note, that using the parametrization  $u^k(t) = \sum_n b_n^{(k)} \phi_n^{(k)}(t)$ , we may precalculate the various integrals

over the basis functions  $\phi_n^{(k)}$ , which allows for significantly faster computation. We elaborate further on this in Appendix A. Each increasing term in the Magnus expansion grows in complexity, hence, we must for all practical purposes truncate the Magnus expansion at some finite term  $m$ . Here the per step error  $\|\Omega_j - \sum_{n=1}^m \Omega_j^{[n]}\|$  scales as  $\mathcal{O}(\Delta t^{2m+1})$  and the accumulated error in the final state  $|\psi(T)\rangle$  scales as  $\mathcal{O}(\Delta t^{2m})$  [46]. Note that written in the form of Eq. (2) and (4), we may also pre-calculate the commutators, which again allows for faster computation.

In the context of optimization, gradient-based methods typically outperform gradient-free alternatives [63]. In our case, we may obtain the derivatives by using the multi-variate chain-rule similarly to Refs. [44, 63],

$$\begin{aligned} \frac{\partial \mathcal{F}}{\partial b_n^{(k)}} = & \sum_j \left( \frac{\partial \mathcal{F}}{\partial c_{k,j}^{(1)}} \frac{\partial c_{k,j}^{(1)}}{\partial b_n^{(k)}} + \frac{\partial \mathcal{F}}{\partial c_{k,j}^{(2)}} \frac{\partial c_{k,j}^{(2)}}{\partial b_n^{(k)}} \right. \\ & \left. + \sum_{k' < k} \frac{\partial \mathcal{F}}{\partial c_{k',k,j}^{(3)}} \frac{\partial c_{k',k,j}^{(3)}}{\partial b_n^{(k)}} + \sum_{k' > k} \frac{\partial \mathcal{F}}{\partial c_{k,k',j}^{(3)}} \frac{\partial c_{k,k',j}^{(3)}}{\partial b_n^{(k)}} + \dots \right). \end{aligned} \quad (7)$$

Here the derivatives  $\partial \mathcal{F} / \partial c_{k,j}^{(1)}$ ,  $\partial \mathcal{F} / \partial c_{k,j}^{(2)}$ ,  $\dots$  are calculable using standard GRAPE propagation [60, 61].

In this work, we benchmark four different integration schemes for quantum control: two-second order methods with one explicitly calculating  $\Omega_j^{[1]}$  (M2exact) and one approximating it via midpoint interpolation (M2approx). As well, we study two fourth-order methods with one explicitly calculating  $\Omega_j^{[1]} + \Omega_j^{[2]}$  (M4exact) and one approximating it via Gauss–Legendre quadrature (M4approx). Note, that M2approx and M4approx have previously been used as numerical integration schemes [46], while M2approx may readily be seen as the current standard in the quantum control literature [20, 59–61, 63]. We elaborate on the derivation of these methods in Appendix A.

### III. RESULTS

#### A. Controlling a spin chain within the RWA

To compare the different methods, we consider control of a one-dimensional spin chain where we model an Ising-type spin-spin interaction for nearest and next-nearest neighboring spins, which was also studied recently in Refs. [27, 43]. We assume access to two independent global control fields  $u^{(x)}$  and  $u^{(y)}$  orthogonal to the chain and driven at qubit-resonance. With this, the drift Hamiltonian becomes

$$H_0 = \frac{1}{2} \sum_j \omega_j \sigma_j^z - J \sum_j \sigma_j^z \sigma_{j+1}^z - g \sum_j \sigma_j^z \sigma_{j+2}^z, \quad (8)$$

where  $J$  is the nearest spin-spin interaction,  $g = J/10$  is the next-nearest spin-spin interaction, and  $\sigma$  denotes the Pauli spin operator. Here we model periodic boundary conditions and assume an isotropic spin chain ( $\omega = \omega_j$  for all  $j$ ). The control part of the Hamiltonian is

$$H_c(t) = 2 \sum_{k=x,y} u^{(k)}(t) \cos(\omega t) \sum_j \sigma_j^k \quad (9)$$

such that  $H(t) = H_0 + H_c(t)$ . We may derive an effective Hamiltonian by using the rotating wave approximation (RWA)

$$\begin{aligned} H_{\text{RWA}}(t) = & -J \sum_j \sigma_j^z \sigma_{j+1}^z - g \sum_j \sigma_j^z \sigma_{j+2}^z \\ & + \sum_{k=x,y} u^{(k)}(t) \sum_j \sigma_j^k. \end{aligned} \quad (10)$$

We express the control pulses in a modulated Fourier basis  $\phi_n^{(k)}(t) = s(t) \cos(\pi n t / T)$  and  $\phi_n^{(k)}(t) = s(t) \sin(\pi n t / T)$  for even and odd values of  $n = 1, 2, \dots, 8$ , respectively, and  $k = x, y$ . Here the modulation function  $s(t)$  denotes a shape function that enforces the pulse to smoothly start and end at zero

$$s(t) = \begin{cases} \frac{1}{2} [\cos(\pi(\frac{t}{\tau} - 1)) + 1], & \text{for } 0 \leq t < \tau, \\ 1 & \text{for } \tau \leq t < T - \tau, \\ \frac{1}{2} [\cos(\pi(\frac{t-T}{\tau} + 1)) + 1] & \text{for } T - \tau \leq t \leq T. \end{cases} \quad (11)$$

For optimization we use a sequential programming (least squares) algorithm [66] implemented in the Python library Scipy [67]. This optimization algorithm allows us to handle non-linear constraints of the form

$$u_{\min}^{(k)} \leq u^{(k)}(t) \leq u_{\max}^{(k)} \text{ for all } k, t, \quad (12)$$

with  $u_{\min}^{(k)}$  and  $u_{\max}^{(k)}$  denoting the minimal and maximal permissible control fields, respectively, which in this work we choose as  $u_{\max}^{(k)} = -u_{\min}^{(k)} = J$  for  $k = x, y$ .

We seek to make a state transfer between two degenerate ground states from an initial state  $|\psi_0\rangle = |0, 0, \dots, 0\rangle$  and a target state  $|\psi_t\rangle = |1, 1, \dots, 1\rangle$ , which requires temporarily populating a set of excited states by the control fields. This task is solvable by minimizing the infidelity of the transfer

$$\mathcal{F} = 1 - |\langle \psi_0 | \psi(T) \rangle|^2, \quad (13)$$

where  $|\psi(T)\rangle$  denotes the solution to the Schrödinger equation from the initial state  $|\psi_0\rangle = |\psi(t=0)\rangle$ .

In the following, we compare the various integration methods for both simulation and control. In order to facilitate such an analysis, we initiate a three step procedure: i) We draw 100 seeds (initial random guesses) and optimize these using a large number of time steps,  $N$ , in order to estimate the “true” infidelity  $\mathcal{F}_{\text{true}}$  at  $TJ = 2.9$ , which for the best solutions lead to an infidelity around

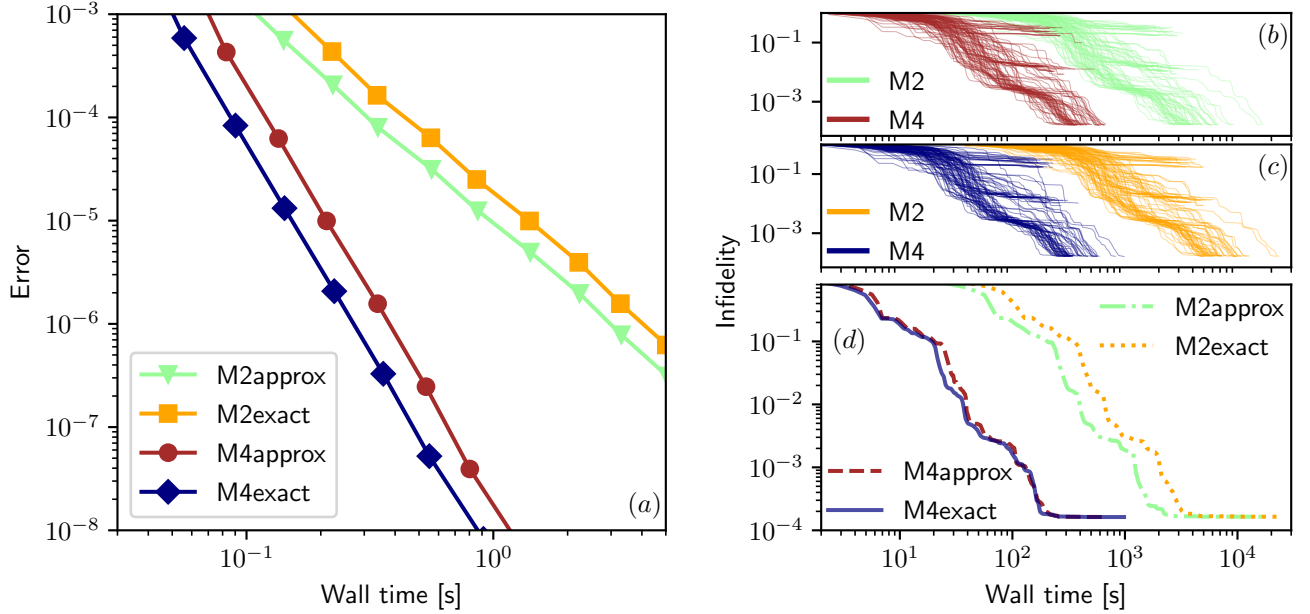


FIG. 2. (a) The wall time consumption for calculating the infidelity for a state transfer on a spin chain without the rotating wave approximation plotted against the numerical error of the infidelity averaged over 100 optimized pulses for the different methods presented in the text. We obtained the data by scanning over different values of  $\Delta t$ , see Fig. 3(a). From this data, we find the  $\Delta t$  that leads to an average error of  $10^{-6}$ . In (b), we compare the optimization from the found discretization of the two approximation methods. We repeat in (c) the comparison for the two exact methods. In (d), we depict the smallest infidelity at each wall time duration for each of the different methods.

$10^{-4}$ . ii) Using the optimized pulses, we now scan over different values of  $\Delta t$  in order to calculate the infidelity  $\mathcal{F}_{\text{calculated}}(\Delta t)$ . For each  $\Delta t$  we further calculate the simulation error  $|\mathcal{F}_{\text{calculated}}(\Delta t) - \mathcal{F}_{\text{true}}|$  and monitor the wall time (i.e., computational time). We depict in Fig. 1(a) the average simulation error as a function of the average wall time for the various methods. From the figure, we observe an excellent improvement in using the two fourth-order methods, which provides around a factor of 10 in speed up for an average accuracy of  $10^{-6}$ . Interestingly, M2exact performs worse than M2approx, while M4exact performs better than M4approx. We depict the results of the  $\Delta t$  scan and the initialization time for each method in Fig. 3. iii) At last, we also compare the various methods for control optimization. From the obtained data, we estimate for each integration scheme the  $\Delta t$  that on average leads to a simulation error of  $10^{-6}$ . Using the found  $\Delta t$ , we then optimize the 100 seeds used in step i) again, where we now save the infidelity and wall time for each incremental update made by GRAPE. We depict the optimization trajectories (reached infidelity versus wall time) in Fig. 1(b) and Fig. 1(c) for the two approximation and the two exact methods, respectively. For an easy comparison, we further depict in Fig. 1(d) the smallest infidelity at each wall time instance for each of the different methods. Again, we observe around a factor of 10 speedup with the fourth-order methods compared to the second order methods.

## B. Controlling a spin chain without the RWA

We now make an additional comparison, where we seek to simulate and optimize the spin chain without the rotating wave approximation. This is easily achievable by including the cosine drives from Eq. (9) into our basis functions  $\phi_n^{(k)}(t) \rightarrow \phi_n^{(k)}(t) \cos(\omega t)$ . Not having the rotating wave approximation requires a larger number of time steps  $N$  to resolve the fast oscillations from the external fields, making simulations typically slow. In this section, we model a resonance frequency of  $\omega = 20J$ , which is in a regime [44] where the rotating wave approximation typically leads to errors compatible with the previously optimized infidelities. In other words, this is a regime where we need the more exact model in realistic simulations.

We now repeat the procedure from the previous section in this new scenario. In Fig. 2(a), we depict the simulation error versus the wall time for each of the four methods averaged over 100 optimized pulses. Overall we see the same tendencies as before: we obtain around a factor of 10 speed up with the fourth-order methods relative to the second-order ones. We still observe the counter-intuitive tendency that M2exact performs worse than M2approx. In Fig. 2(b) and Fig. 2(c) we depict the optimization trajectories for the approximate and the exact methods, respectively. Similarly to before, we also depict in Fig. 2(d) the smallest infidelity at each wall time instance. We again observe a factor of 10 in speed

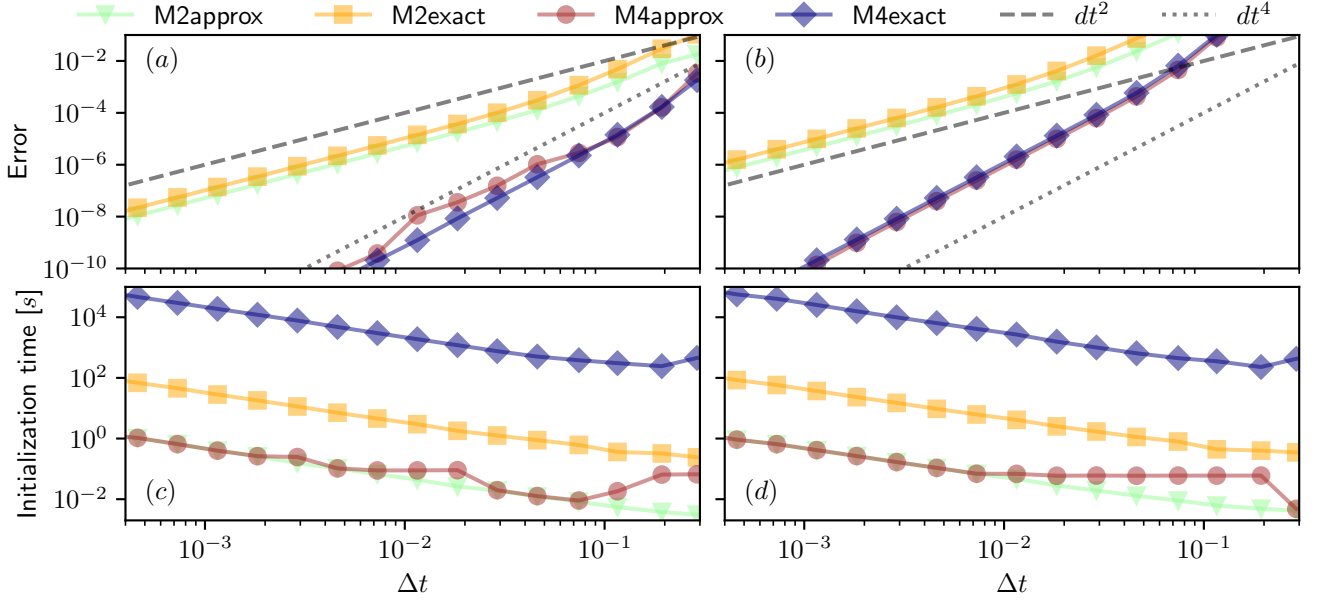


FIG. 3. The error of time propagation at various values of  $\Delta t$  for (a) with and (b) without the RWA. Here we observe that each method is consistent with its analytically predicted error scaling. We also depict the initialization times for (c) with and (d) without the RWA. For the two exact methods, we pre-calculate the integrals (2)-(6) numerically and note that, where possible, calculating these analytically further reduces this initialization overhead.

improvement with the two fourth-order methods for optimization.

### C. Further comparison and discussion

Before concluding, we briefly elaborate on the differences between the various methods introduced and benchmarked in the preceding sections. First, we depict the aforementioned  $\Delta t$ -scans in Fig. 3(a) and (b) with and without the RWA, respectively. Here we observe that each method is consistent with the second and fourth-order scaling also marked in the figures.

We also depict the initialization time for each method in Fig. 3(c) and (d) with and without the RWA, respectively. Note that we pre-evaluate the sampling points for the two approximation methods, while for the two exact methods, we pre-calculate the integrals. In addition, we also pre-calculate the commutators for the two fourth-order methods. The most expensive method is by far M4exact. However, we believe the initialization time is heavily reducible for a large variety of control settings by pre-calculating the integrals analytically but at the price of overhead in human labor. Nonetheless, since M4exact is the consistently fastest method, there are many scenarios where this additional overhead is far smaller than the optimization time, including where many noise trajectories must be sampled, where search complexity requires many different initial seeds, or where Hilbert space complexity makes matrix exponentiation far more expensive than the integrals themselves.

## IV. CONCLUSION

In this work, we have derived a new quantum optimal control framework based on improved time propagation using a discretized Magnus expansion. We obtained several high-performing quantum control propagators within this framework, which we tested in equal-accuracy comparisons to state-of-the-art approaches. In doing so, we demonstrated around an order of magnitude in speedup for both fast and slow system dynamics relative to the timescale of the control modulation. In particular, we derived an exact fourth-order Magnus propagator (M4exact) that is consistently faster than the previous methods for individual runs, though at an upfront overhead cost. At the same time, the Gauss-Legendre quadrature approximation (M4approx) offers a slight reduction in speedup while dramatically reducing this overhead. The overhead in precomputing commutators and integrals typically represents a small fraction of the entire computation time for standard optimal control problems. Still, the appropriate method can always be chosen accordingly. We foresee this new approach to have widespread applicability in optimal control-theoretic settings, and wherever many dynamical trajectories must be calculated, such as for Monte Carlo sampling.

## ACKNOWLEDGMENTS

We thank Francesco Preti and Michael Schilling for helpful discussions. This work was funded by the Carls-

berg Foundation, the Deutsche Forschungsgemeinschaft (DFG, German Research Foundation) under Germany's Excellence Strategy – Cluster of Excellence Matter and Light for Quantum Computing (ML4Q) EXC 2004/1 – 390534769, and through the European Union's Horizon 2020 research and innovation programme under Grant

Agreements No. 817482 (PASQuanS) and No. 820394 (ASTERIQS). The numerical results presented in this work were obtained at the Centre for Scientific Computing, Aarhus, phys.au.dk/forskning/cscaa.

## Appendix A: Different methods

### 1. M2exact

The first propagation scheme we consider is calculating the exact first term in the Magnus expansion. Here (and in the following methods), we start by shifting the time scale  $[t_j, t_j + \Delta t]$  to  $[0, \Delta t]$ . In this case, we may evaluate Eq. (3) by using the parametrization  $u^k(t) = \sum_n b_n^{(k)} \phi_n^{(k)}(t)$

$$c_{k,j}^{(1)} = \sum_n b_n^{(k)} \int_0^{\Delta t} \phi_n^{(k)}(t_j + t_1) dt_1, \quad (\text{A1})$$

with derivative

$$\frac{\partial c_{k,j}^{(1)}}{b_n^{(k)}} = \int_0^{\Delta t} \phi_n^{(k)}(t_j + t_1) dt_1. \quad (\text{A2})$$

This integrals may be calculated in advance either analytically or numerically to arbitrary precision. In this work we calculated the integrals numerically.

### 2. M2approx (standard GRAPE)

The second scheme we consider is the current standard in literature: GRAPE, which is done by using midpoint interpolation of Eq. (A1) [46], which gives the coefficient

$$c_{k,j}^{(1)} = \Delta t \sum_n b_n^{(k)} \phi_n^{(k)}(t_j + \Delta t/2), \quad (\text{A3})$$

with derivative given as in [44] by

$$\frac{\partial c_{k,j}^{(1)}}{b_n^{(k)}} = \Delta t \phi_n^{(k)}(t_j + \Delta t/2). \quad (\text{A4})$$

### 3. M4exact

The first term in the Magnus expansion has already been calculated so we just need to evaluate Eq. (5) and (6). Then,

$$c_{k,j}^{(2)} = \frac{1}{2} \sum_n b_n^{(k)} \int_0^{\Delta t} \left( \int_0^{t_1} \phi_n^{(k)}(t_j + t_2) dt_2 - \phi_n^{(k)}(t_j + t_1) t_1 \right) dt_1, \quad (\text{A5})$$

with derivative

$$\frac{\partial c_{k,j}^{(2)}}{\partial b_n^{(k)}} = \frac{1}{2} \int_0^{\Delta t} \left( \int_0^{t_1} \phi_n^{(k)}(t_j + t_2) dt_2 - \phi_n^{(k)}(t_j + t_1) t_1 \right) dt_1. \quad (\text{A6})$$

Lastly we have

$$c_{k,k',j}^{(3)} = \frac{1}{2} \sum_{n,m} \left[ b_n^{(k)} b_m^{(k')} \int_0^{\Delta t} \left( \phi_n^{(k)}(t_j + t_1) \int_0^{t_1} \phi_m^{(k')}(t_j + t_2) dt_2 \right) dt_1 \right. \\ \left. - b_n^{(k')} b_m^{(k)} \int_0^{\Delta t} \left( \phi_m^{(k')}(t_j + t_1) \int_0^{t_1} \phi_n^{(k)}(t_j + t_2) dt_2 \right) dt_1 \right], \quad (\text{A7})$$

with derivative

$$\frac{\partial c_{k,k',j}^{(3)}}{\partial b_l^{(h)}} = \begin{cases} \frac{1}{2} \sum_m b_m^{(k')} \int_0^{\Delta t} \left( \phi_n^{(k)}(t_j + t_1) \int_0^{t_1} \phi_m^{(k')}(t_j + t_2) dt_2 \right) dt_1 & \text{if } l = n \text{ and } h = k \\ \frac{1}{2} \sum_n b_n^{(k)} \int_0^{\Delta t} \left( \phi_n^{(k)}(t_j + t_1) \int_0^{t_1} \phi_m^{(k')}(t_j + t_2) dt_2 \right) dt_1 & \text{if } l = m \text{ and } h = k' \\ -\frac{1}{2} \sum_m b_m^{(k)} \int_0^{\Delta t} \left( \phi_m^{(k')}(t_j + t_1) \int_0^{t_1} \phi_n^{(k)}(t_j + t_2) dt_2 \right) dt_1 & \text{if } l = n \text{ and } h = k' \\ -\frac{1}{2} \sum_n b_n^{(k')} \int_0^{\Delta t} \left( \phi_m^{(k')}(t_j + t_1) \int_0^{t_1} \phi_n^{(k)}(t_j + t_2) dt_2 \right) dt_1 & \text{if } l = m \text{ and } h = k \end{cases} \quad (\text{A8})$$

#### 4. M4approx

The last method we consider is an approximation scheme of fourth order based on approximating the integral with Gaussian-Legendre quadratures [46]. We define  $H_{1,2} = H(t_j + c_{1,2}\Delta t)$  and  $u_{1,2}^{(k)} = u^{(k)}(t_j + c_{1,2}\Delta t)$  where  $c_{1,2} = 1/2 \mp \sqrt{3}/6$ . With this the Magnus expansion reads

$$\Omega_j = \frac{\Delta t}{2} (H_1 + H_2) - i \frac{\sqrt{3}}{12} \Delta t^2 [H_2, H_1] \\ = \Delta t H_0 + \Delta t \sum_k \frac{u_1^{(k)} + u_2^{(k)}}{2} H_k \quad (\text{A9})$$

$$- i \frac{\sqrt{3}}{12} \Delta t^2 \left( \sum_k (u_1^{(k)} - u_2^{(k)}) [H_0, H_k] + \sum_{k < k'} (u_2^{(k)} u_1^{(k')} - u_2^{(k')} u_1^{(k)}) [H_k, H_{k'}] \right). \quad (\text{A10})$$

With this we have the coefficient

$$c_{k,j}^{(1)} = \Delta t \frac{u_1^{(k)} + u_2^{(k)}}{2} = \Delta t \sum_n b_n^{(k)} \frac{\phi_n^{(k)}(t_1) + \phi_n^{(k)}(t_2)}{2}, \quad (\text{A11})$$

where we have introduced the notation  $t_{1,2} = t_j + c_{1,2}\Delta t$ . The derivative is

$$\frac{\partial c_{k,j}^{(1)}}{b_n^{(k)}} = \Delta t \frac{\phi_n^{(k)}(t_1) + \phi_n^{(k)}(t_2)}{2}. \quad (\text{A12})$$

Then

$$c_{k,j}^{(2)} = \frac{\sqrt{3}}{12} \Delta t^2 (u_1^{(k)} - u_2^{(k)}) = \frac{\sqrt{3}}{12} \Delta t^2 \sum_b b_n^{(k)} (\phi_n^{(k)}(t_1) - \phi_n^{(k)}(t_2)), \quad (\text{A13})$$

with derivative

$$\frac{\partial c_{k,j}^{(2)}}{b_n^{(k)}} = \frac{\sqrt{3}}{12} \Delta t^2 (\phi_n^{(k)}(t_1) - \phi_n^{(k)}(t_2)). \quad (\text{A14})$$

And

$$c_{k,k',j}^{(3)} = \frac{\sqrt{3}}{12} \Delta t^2 (u_2^{(k)} u_1^{(k')} - u_2^{(k')} u_1^{(k)}) \quad (\text{A15})$$

$$= \frac{\sqrt{3}}{12} \Delta t^2 \sum_{n,m} b_n^{(k)} b_m^{(k')} \phi_n^{(k)}(t_2) \phi_m^{(k')}(t_1) - b_n^{(k')} b_m^{(k)} \phi_n^{(k')}(t_2) \phi_m^{(k)}(t_1), \quad (\text{A16})$$

with derivative

$$\frac{\partial c_{k,k',j}^{(3)}}{\partial b_l^{(h)}} = \begin{cases} \frac{\sqrt{3}}{12} \Delta t^2 \sum_m b_m^{(k')} \phi_n^{(k)}(t_2) \phi_m^{(k')}(t_1) & \text{if } l = n \text{ and } h = k \\ \frac{\sqrt{3}}{12} \Delta t^2 \sum_n b_n^{(k)} \phi_n^{(k)}(t_2) \phi_m^{(k')}(t_1) & \text{if } l = m \text{ and } h = k' \\ -\frac{\sqrt{3}}{12} \Delta t^2 \sum_m b_m^{(k)} \phi_n^{(k')}(t_2) \phi_m^{(k')}(t_1) & \text{if } l = n \text{ and } h = k' \\ -\frac{\sqrt{3}}{12} \Delta t^2 \sum_n b_n^{(k')} \phi_n^{(k')}(t_2) \phi_m^{(k)}(t_1) & \text{if } l = m \text{ and } h = k \end{cases} \quad (\text{A17})$$

- 
- [1] E. Farhi, J. Goldstone, and S. Gutmann, arXiv preprint arXiv:1411.4028 (2014).
- [2] A. W. Harrow, A. Hassidim, and S. Lloyd, Phys. Rev. Lett. **103**, 150502 (2009).
- [3] A. Peruzzo, J. McClean, P. Shadbolt, M.-H. Yung, X.-Q. Zhou, P. J. Love, A. Aspuru-Guzik, and J. L. O'Brien, Nature communications **5**, 1 (2014).
- [4] J. R. McClean, J. Romero, R. Babbush, and A. Aspuru-Guzik, New J. Phys. **18**, 023023 (2016).
- [5] M. Schuld, I. Sinayskiy, and F. Petruccione, Contemporary Physics **56**, 172 (2015).
- [6] J. Biamonte, P. Wittek, N. Pancotti, P. Rebentrost, N. Wiebe, and S. Lloyd, Nature **549**, 195 (2017).
- [7] A. M. Dalzell, A. W. Harrow, D. E. Koh, and R. L. La Placa, Quantum **4**, 264 (2020).
- [8] S. Boixo, V. N. Smelyanskiy, A. Shabani, S. V. Isakov, M. Dykman, V. S. Denchev, M. H. Amin, A. Y. Smirnov, M. Mohseni, and H. Neven, Nature communications **7**, 1 (2016).
- [9] A. Kandala, A. Mezzacapo, K. Temme, M. Takita, M. Brink, J. M. Chow, and J. M. Gambetta, Nature **549**, 242 (2017).
- [10] C. Kokail, C. Maier, R. van Bijnen, T. Brydges, M. K. Joshi, P. Jurcevic, C. A. Muschik, P. Silvi, R. Blatt, C. F. Roos, *et al.*, Nature **569**, 355 (2019).
- [11] A. Omran, H. Levine, A. Keesling, G. Semeghini, T. T. Wang, S. Ebadi, H. Bernien, A. S. Zibrov, H. Pichler, S. Choi, *et al.*, Science **365**, 570 (2019).
- [12] M. P. Harrigan, K. J. Sung, M. Neeley, K. J. Satzinger, F. Arute, K. Arya, J. Atalaya, J. C. Bardin, R. Barends, S. Boixo, *et al.*, Nature Physics **17**, 332 (2021).
- [13] D. d'Alessandro, *Introduction to quantum control and dynamics* (Chapman and Hall/CRC, 2007).
- [14] J. Werschnik and E. Gross, Journal of Physics B: Atomic, Molecular and Optical Physics **40**, R175 (2007).
- [15] S. J. Glaser, U. Boscain, T. Calarco, C. P. Koch, W. Köckenberger, R. Kosloff, I. Kuprov, B. Luy, S. Schirmer, T. Schulte-Herbrüggen, *et al.*, The European Physical Journal D **69**, 1 (2015).
- [16] D. Dong, C.-C. Shu, J. Chen, X. Xing, H. Ma, Y. Guo, and H. Rabitz, IEEE Transactions on Control Systems Technology (2020).
- [17] J. J. Sørensen, J. S. Nyemann, F. Motzoi, J. Sherson, and T. Vosegaard, The Journal of Chemical Physics **152**, 054104 (2020).
- [18] M. M. Müller, R. S. Said, F. Jelezko, T. Calarco, and S. Montangero, arXiv preprint arXiv:2104.07687 (2021).
- [19] D. Goodwin and I. Kuprov, The Journal of chemical physics **144**, 204107 (2016).
- [20] M. Dalgaard, F. Motzoi, J. H. M. Jensen, and J. Sherson, Phys. Rev. A **102**, 042612 (2020).
- [21] J. H. M. Jensen, F. S. Møller, J. J. Sørensen, and J. F. Sherson, Phys. Rev. A **103**, 062612 (2021).
- [22] J. H. M. Jensen, F. S. Møller, J. J. Sørensen, and J. F. Sherson, arXiv preprint arXiv:2008.06076 (2020).
- [23] M. M. Müller, S. Gherardini, and F. Caruso, Scientific reports **8**, 1 (2018).
- [24] B.-J. Liu, X.-K. Song, Z.-Y. Xue, X. Wang, and M.-H. Yung, Phys. Rev. Lett. **123**, 100501 (2019).
- [25] B. Khani, S. T. Merkel, F. Motzoi, J. M. Gambetta, and F. K. Wilhelm, Phys. Rev. A **85**, 022306 (2012).
- [26] R. S. Gupta, C. L. Edmunds, A. R. Milne, C. Hempel, and M. J. Biercuk, npj Quantum Information **6**, 1 (2020).
- [27] M. Dalgaard, C. A. Weidner, and F. Motzoi, arXiv preprint arXiv:2107.11388 (2021).
- [28] P. Palitapongarnpim, P. Wittek, E. Zahedinejad, S. Vedaie, and B. C. Sanders, Neurocomputing **268**, 116 (2017).
- [29] M. Bukov, A. G. Day, D. Sels, P. Weinberg, A. Polkovnikov, and P. Mehta, Phys. Rev. X **8**, 031086 (2018).
- [30] H. Xu, J. Li, L. Liu, Y. Wang, H. Yuan, and X. Wang, npj Quantum Information **5**, 1 (2019).
- [31] Z. An and D. Zhou, EPL (Europhysics Letters) **126**, 60002 (2019).
- [32] M. Dalgaard, F. Motzoi, J. J. Sørensen, and J. Sherson, npj Quantum Information **6**, 1 (2020).
- [33] J. Yao, M. Bukov, and L. Lin, in *Mathematical and Scientific Machine Learning* (PMLR, 2020) pp. 605–634.
- [34] Y. Baum, M. Amico, S. Howell, M. Hush, M. Liuzzi, P. Mundada, T. Merkh, A. R. Carvalho, and M. J. Biercuk, arXiv preprint arXiv:2105.01079 (2021).
- [35] K. Mitarai, M. Negoro, M. Kitagawa, and K. Fujii, Phys. Rev. A **98**, 032309 (2018).
- [36] F. Motzoi, M. P. Kaicher, and F. K. Wilhelm, Phys. Rev. Lett. **119**, 160503 (2017).
- [37] J. M. Arrazola, T. R. Bromley, J. Izaac, C. R. Myers, K. Brádler, and N. Killoran, Quantum Science and Technology **4**, 024004 (2019).
- [38] H. Chen, H. Li, F. Motzoi, L. Martin, K. B. Whaley, and M. Sarovar, New J. Phys. **22**, 113014 (2020).
- [39] L. Magrini, P. Rosenzweig, C. Bach, A. Deutschmann-Olek, S. G. Hofer, S. Hong, N. Kiesel, A. Kugi, and M. Aspelmeyer, Nature **595**, 373 (2021).
- [40] F. Motzoi, E. Halperin, X. Wang, K. B. Whaley, and S. Schirmer, Phys. Rev. A **94**, 032313 (2016).
- [41] D. Basilewitsch, F. Cosco, N. L. Gullo, M. Möttönen, T. Ala-Nissilä, C. P. Koch, and S. Maniscalco, New J. Phys. **21**, 093054 (2019).
- [42] B. Koczor and S. C. Benjamin, arXiv preprint arXiv:2008.13774 (2020).
- [43] M. Dalgaard, F. Motzoi, and J. Sherson, arXiv preprint arXiv:2107.00008 (2021).
- [44] F. Motzoi, J. M. Gambetta, S. Merkel, and F. Wilhelm, Phys. Rev. A **84**, 022307 (2011).



- [45] W. Magnus, Communications on pure and applied mathematics **7**, 649 (1954).
- [46] S. Blanes, F. Casas, J.-A. Oteo, and J. Ros, Physics reports **470**, 151 (2009).
- [47] N. Auer, L. Einkemmer, P. Kandolf, and A. Ostermann, Computer Physics Communications **228**, 115 (2018).
- [48] A. Ma, A. B. Magann, T.-S. Ho, and H. Rabitz, Phys. Rev. A **102**, 013115 (2020).
- [49] M. Plischke and B. Bergersen, *Equilibrium statistical physics* (World Scientific, 1994).
- [50] J. I. Cirac and P. Zoller, Phys. Rev. Lett. **74**, 4091 (1995).
- [51] I. Bloch, Nature **453**, 1016 (2008).
- [52] A. Blais, S. M. Girvin, and W. D. Oliver, Nature Physics **16**, 247 (2020).
- [53] X. Wu, X. Liang, Y. Tian, F. Yang, C. Chen, Y.-C. Liu, M. K. Tey, and L. You, Chinese Physics B (2020).
- [54] A. Kinos, D. Hunger, R. Kolesov, K. Mølmer, H. de Riedmatten, P. Goldner, A. Tallaïre, L. Morvan, P. Berger, S. Welinski, *et al.*, arXiv preprint arXiv:2103.15743 (2021).
- [55] A. G. Fowler, M. Mariantoni, J. M. Martinis, and A. N. Cleland, Phys. Rev. A **86**, 032324 (2012).
- [56] R. Barends, J. Kelly, A. Megrant, A. Veitia, D. Sank, E. Jeffrey, T. C. White, J. Mutus, A. G. Fowler, B. Campbell, *et al.*, Nature **508**, 500 (2014).
- [57] M. Christandl, N. Datta, A. Ekert, and A. J. Landahl, Phys. Rev. Lett. **92**, 187902 (2004).
- [58] M.-H. Yung, Phys. Rev. A **74**, 030303 (2006).
- [59] S. Machnes, U. Sander, S. J. Glaser, P. De Fouquières, A. Gruslys, S. Schirmer, and T. Schulte-Herbrüggen, Phys. Rev. A **84**, 022305 (2011).
- [60] N. Khaneja, T. Reiss, C. Kehlet, T. Schulte-Herbrüggen, and S. J. Glaser, Journal of magnetic resonance **172**, 296 (2005).
- [61] P. De Fouquieres, S. Schirmer, S. Glaser, and I. Kuprov, Journal of Magnetic Resonance **212**, 412 (2011).
- [62] T. Schulte-Herbrüggen, A. Spörl, N. Khaneja, and S. Glaser, Journal of Physics B: Atomic, Molecular and Optical Physics **44**, 154013 (2011).
- [63] J. Sørensen, M. Aranburu, T. Heinzel, and J. Sherson, Phys. Rev. A **98**, 022119 (2018).
- [64] T. Caneva, T. Calarco, and S. Montangero, Phys. Rev. A **84**, 022326 (2011).
- [65] S. van Frank, M. Bonneau, J. Schmiedmayer, S. Hild, C. Gross, M. Cheneau, I. Bloch, T. Pichler, A. Negretti, T. Calarco, *et al.*, Scientific reports **6**, 34187 (2016).
- [66] D. Kraft, DFVLR Obersaffeuhofen, Germany (1988).
- [67] P. Virtanen, R. Gommers, T. E. Oliphant, M. Haberland, T. Reddy, D. Cournapeau, E. Burovski, P. Peterson, W. Weckesser, J. Bright, *et al.*, Nature methods **17**, 261 (2020).